detritus | Multidisciplinary Journal for Circular Economy and Sustainable Management of Residues

CISA

INFLUENCE OF IMPURITY ELEMENTS ON THE CASTABILITY OF RECYCLED 6XXX SERIES AL ALLOYS

Emidio Giansante *, Alberto Fabrizi and Giulio Timelli

Department of Management and Engineering, University of Padova, Stradella San Nicola 3, 36100 Vicenza, Italy

Article Info:
Received:
24 June 2025
Accepted:
29 July 2025
Available online:
16 September 2025

Keywords:
Hot tearing susceptibility
Kou's criterion
CRC test
6xxx series Al alloys

ABSTRACT

Hot tearing represents a relevant limitation to castability, particularly in wrought aluminum alloys having a wide solidification range. To assess the alloy's vulnerability to hot tearing, a variety of predictive models and testing methodologies have been developed. This study aims to validate the Kou model through the comparison of experimental data obtained using the Constrained Rod Casting (CRC) test on selected 6XXX series Al alloys. Additionally, the investigations explore the influence of microstructural features and phase constituents on the formation of hot tears. The results indicate that the sensitivity to hot tears is higher in alloys with 0.2 wt% Fe and decreases by increasing iron content. The α-$Al_{15}(Fe,Mn)_3Si_2$ phase appears to promote grain coalescence, facilitating bridging between primary dendrites and, thereby, improving the castability of the alloy. Furthermore, the study suggests that thermodynamic simulation and the application of Kou index can offer valuable insights into the casting of alloys. These findings will contribute to the identification of optimized alloy chemistries suitable for producing near-net-shape components using casting techniques traditionally applied to Al casting.

1. INTRODUCTION

The automotive and aerospace industry is increasingly turning to aluminum alloys (Graf, 2021) for their favorable properties, such as high strength-to-weight ratio, good corrosion resistance, easy formability and, theoretically, indefinite recycling capability (Van den Eynde, et al., 2022). This transition aligns with industry goals to reduce greenhouse gas emissions (Raabe, et al., 2022), dependence on critical raw materials (Ferro & Bonollo, 2023) and overall energy consumption (Cui & Roven, 2010).

However, replacing steel with aluminum presents challenges, particularly because casting aluminum alloys often offer lower mechanical performance required for structural applications. This limitation has led to a growing interest in wrought alloys which offer superior mechanical properties and are now being considered for near-net-shape casting applications (Poznak, Freiberg, & Sanders, 2018). However, using wrought alloys in conventional casting processes remains complex.

These alloys typically exhibit narrow compositional tolerances and broad solidification ranges (Phillion, Thompson, Crockcroft, & Wells, 2008) both of which adversely affect castability, i.e. the ability to be successfully cast into complex shapes without defect formation (Eskin, Suytno, & Katgerman, 2004). Among the various solidification-related defects, hot tearing (also known as hot cracking) represents a relevant limitation to castability, particularly in wrought alloys having a wide solidification range which increases their susceptibility to thermal contraction.

During the solidification process, these alloys can accumulate internal tensile stress and when the semi-solid metal cannot accommodate these tensile strains, interdendritic cracking, or hot tearing, is likely to form (Dhale & StJohn, 1998). This phenomenon is considered to be one of the most critical and complex defect in casting, resulting from the interaction between multiple factors such as mass flow, thermal gradients, and fluid flow (Eskin, Suytno, & Katgerman, 2004), making analysis and prediction challenging.

As described in the pioneering work of Rappaz and Drezet (Rappaz, Drezet, & Gremaud, 1999), hot tears occur especially due to the constrained contraction in the mushy zone, where the lack of liquid feeding can lead to material failure. When the solidification exceeds the dendritic coherence threshold, the primary aluminum phase forms an interconnected solid network, which incorporates liquid pockets within interstitial spaces. As this network solidifies further, the permeability within the solid structure decreases, leading to the so-called interdendritic separation. Furthermore, shrinkage generates porosity, which acts as nucleation sites for hot tears (Uludag, Çetin, Dispinar, & Tiryakioglu, 2018).

* Corresponding author:
Emidio Giansante
email: emidio.giansante@phd.unipd.it

Detritus / Volume 32 - 2025 / pages 67-73
https://doi.org/10.31025/2611-4135/2025.19521

Industrial casting processes typically proceed under non-equilibrium solidification conditions, well described by the Scheil model (Scheil, 1942). Under these non-equilibrium conditions, micro-segregation areas and intermetallic compounds, which have a significant influence on material strength and susceptibility to hot tearing, are more likely to develop. This tendency is particularly pronounced in secondary alloys, which generally contain higher concentrations of alloying elements and impurities.

Consequently, despite the economic and environmental advantages of producing secondary alloys over primary routes, the use of secondary wrought aluminium alloys unfortunately still remains limited due to their high sensitivity to impurity levels introduced through recycling processes.

To assess the vulnerability of an alloy to hot tearing, a variety of predictive models and testing methodologies have been developed. They serve as predictive tools to design casting processes and alloy compositions to minimize defect occurrence. These include both experimental tests, which directly evaluate cracking tendency under controlled conditions and theoretical or semi-empirical models, which are based on thermodynamic and kinetic simulations of alloy solidification behavior.

Due to its simplicity and ease of application, Kou's criterion is one of the most widely used theoretical approach (Kou, 2015): it proposes that hot tearing occurs when the tensile stress exceeds the combined resistance offered by grain growth and liquid feeding. The model introduces a Hot Tearing Susceptibility (HTS) index, defined by the slope of the temperature versus solid fraction curve ($T\ vs\ f_s$), near the final stage of solidification $(f_s \rightarrow 1) : HTS = |\Delta T/\Delta(f_s^{1/2})|$.

In a previous study (Giansante, Timelli & Fabrizi, 2024), the authors applied the Kou criterion to predict how variations in Si, Mg, Fe and Mn concentrations affect hot tearing in 6XXX series aluminum alloys. The current study extends this work by comparing these predictive results with experimental data obtained through the Constrained Rod Casting (CRC) test, a widely used method to qualitatively assess castability and hot tearing tendency in both vertical and horizontal mold configurations.

The CRC test employs gravity casting into a mold with a series of horizontal arms of different lengths but constant diameters. This setup introduces controlled thermal and mechanical constraints that promote the formation of hot tears at specific locations, making it ideal for evaluating alloy performance under realistic conditions.

This study aims to validate the Kou model using CRC experimental results on selected 6XXX series Al alloys and to examine how microstructural features and phase constituents influence hot tearing behavior in functions of different alloy compositions. The findings will support the identification of alloy chemistries suitable for producing near-net-shape components using casting techniques traditionally applied to Al casting alloys.

Ultimately, this work contributes to a deeper understanding of the hot tearing phenomenon and provides guidance for the development of casting processes that enable the use of high-performance wrought aluminum alloys in advanced structural applications.

2. EXPERIMENTAL PROCEDURE

2.1 Materials

Based on the findings of a previous work (Giansante, Timelli, & Fabrizi, Influence of Chemical Composition on the Hot Tearing Susceptibility of Wrought 6005 Aluminum Alloys, 2024), three experimental 6xxx series aluminum alloys with different concentrations of Si, Mg, and impurity elements (Fe and Mn) were selected for testing.

All three alloys were then produced using commercially pure aluminum as base material. About 5 kg of ingot pieces were charged into a SiC crucible and they were melted in an electrical furnace at 750±5°C. After melting, the surface oxide was skimmed and AlFe20, pure Si, pure Mg and AlMn25 master alloys in the form of waffle or wide rod were added to reach the desired chemical composition. After the addition, the molten bath was held in the furnace for 40 minutes to ensure the correct dissolution and the homogeneity. To reduce hydrogen content and improve the quality of the molten bath, the metal was treated with a commercial salt flux. The bath was stirred prior to flux addition, after which the flux was allowed to react for 20 minutes at the processing temperature. Additionally, a degassing treatment was carried out by purging Argon gas through the melt for 20 minutes. The molten bath was then skimmed and stirred before checking the chemical compositions by optical emission spectrometer (Oxford Instruments - Foundry Master Pro). The average concentrations of the chemical elements for the 3 alloys are listed in Table 1. For each alloy, 2 ingots of 1.5 kg each were then cast and subsequently used in the CRC tests.

2.2 Evaluation of Hot Tearing Susceptibility

2.2.1 Kou criterion

The HTS index for each alloy was initially evaluated using Kou's predictive criterion on the solidification curves, $T\ vs\ f_s$, generated through ThermoCalc™ (Andersson, Helander, Höglund, Shi, & Sundman, 2002), a commercial thermodynamic simulation software. The solidification paths were computed using Scheil's non-equilibrium model based on data from the TCAL 7.1 aluminum database (TCAL7 Technical Information, 2020). Each simulation started at the temperature of 750°C with a computing step of 1°C.

TABLE 1: Chemical composition of the experimental alloys (values in wt. %).

Alloy	Si	Fe	Mn	Mg	Others	Al
1	1.35	0.24	0.00	0.83	(0.2)	Bal.
2	1.28	0.22	0.00	1.12	(0.2)	Bal.
3	0.60	0.86	0.63	0.39	(0.2)	Bal.

In the present investigation, the $\Delta T/\Delta(f_s^{1/2})$ approximation index within the solid fraction range of $0.87<f_s<0.94$ was used to calculate the HTS values, as this interval was reported to correlate well with experimental observations in aluminum alloys (Kou, 2015).

2.2.2 CRC test

To experimentally assess hot tearing susceptibility of the three alloys, the Constrained Rod Casting (CRC) mold in Figure 1 was used. The mold design was adapted from various models reported in the literature; Rajagukgug et al. (Rajagukguk, et al., 2024) higlighted the differences between horizontal and vertical CRC molds. A similar approach was used by Liang et al. (Liang, et al., 2024) in their investigation of the influence of chemical composition and grain refiners on aluminum alloys. Furthermore, Cao & Kou (Cao & Kou, 2006) conducted the CRC test on Mg-Al binary alloys while Uludag et al. (Uludag, Çetin, Dispinar , & Tiryakioglu, 2018) chose this approach to assess the correlation between the hot tearing and melt quality. The CRC mold consists of four rods with a diameter of 9.5 mm and variable lengths. Each rod terminates in a ball end, which serves to prevent free contraction due to shrinkage during solidification. The mold design used in this study includes a pouring basin to minimize turbulence during casting, as well as a thermocouple positioned at the intersection point between the sprue axis and the bottom rod axis, allowing for accurate monitoring of mold temperature. The mold was coated with a graphite-based solution. Prior to casting tests, the previously prepared ingots were melted in a crucible at a furnace temperature of 760±5°C. After approximately 60 minutes, the melt was poured into the CRC mold preheated at 220±5°C and the final castings were removed from the mold after 5 minutes. At least three castings were carried out for each alloy, following the same procedure.

Hot tears in the castings were inspected by eye and the HTS index according to the CRC test was calculated using the following equation (Liang, et al., 2024):

$$HTS = \sum_i (w_i * f_i * L_i) \quad (1)$$

where w_i, f_i and, L_i are factors for crack severity, crack location and rod length, respectively. More in details, w_i represents the so-called weighted index, i.e., a severity index for cracks ranging from 1 for hairline cracks to 4 in cases of complete separation of the involved parts, f_i denotes the crack location index and can assume values of 1, 1.5, or 2, depending on whether the crack appears near the sprue, on the ball end, or in the middle of the rod, respectively. Lastly, L_i accounts for the rod length index, which takes the value of 1 for the longest branch and increases up to 4 for the shortest one.

These indices are designed to reflect the susceptibility of a specific rod or areas to crack formation.

The index values are weighted based on the analysis of temperature variations and the resulting thermal strains across different regions of the mold, which show the higher probability of crack formation in the longer branches.

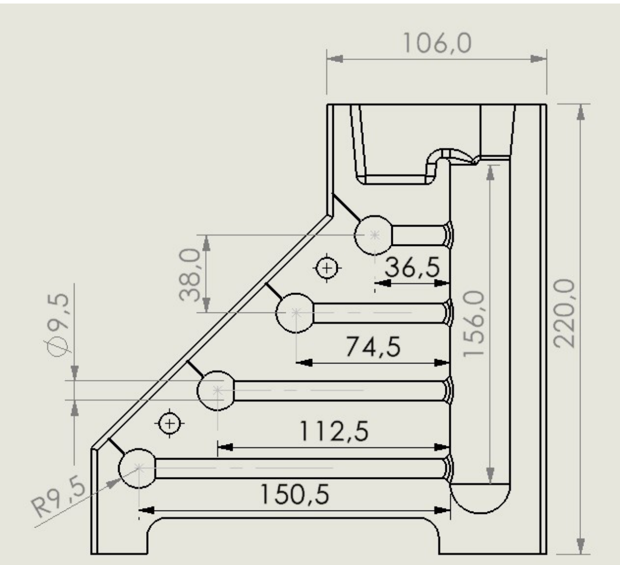

FIGURE 1: Design and dimensions of the CRC mold.

2.3 Microstructural analysis

Microstructural investigations were conducted on specimens drawn from the cross-section of the longest rod of the castings. The specimens were embedded in acrylic resin at room temperature and prepared following standard metallographic procedures, which included grinding with SiC abrasive papers and polishing with a 6 μm diamond paste, followed by final polishing using a colloidal silica suspension.

For grain size evaluation, samples were electrochemically etched using Barker's reagent, and the resulting microstructures were examined using an Optical Microscope (OM) with polarized light; grain sizes were then determined by the linear intercept method. Additionally, the polished samples were examined by Scanning Electron Microscope (SEM) equipped with Energy-Dispersive X-ray Spectroscopy (EDS) to characterize the morphology and chemical composition of intermetallic phases.

3. RESULTS AND DISCUSSION

Figure 2a illustrates the simulated solidification curves for the three investigated alloys. The curves corresponding to Alloy 1 and Alloy 2 are nearly identical, whereas Alloy 3 exhibits a distinct solidification path. This difference can be attributed to the lower Si and Mg contents and significantly higher Fe and Mn concentrations in Alloy 3 compared to the other two alloys, which are chemically similar. All curves display variations in slope, marked by knee points, particularly near the final stages of solidification. The presence of such knee points indicates the precipitation of secondary phases in addition to the primary α-Al phase.

HTS indices were calculated from the solidification curves using Kou's model and the resulting values are presented in the histogram in Figure 2b. Among the three materials, Alloy 1 exhibits the highest vulnerability to the hot tearing. To validate the predictive HTS indices, at least three experimental tests were carried out with the CRC mold and the representing castings of the experimental

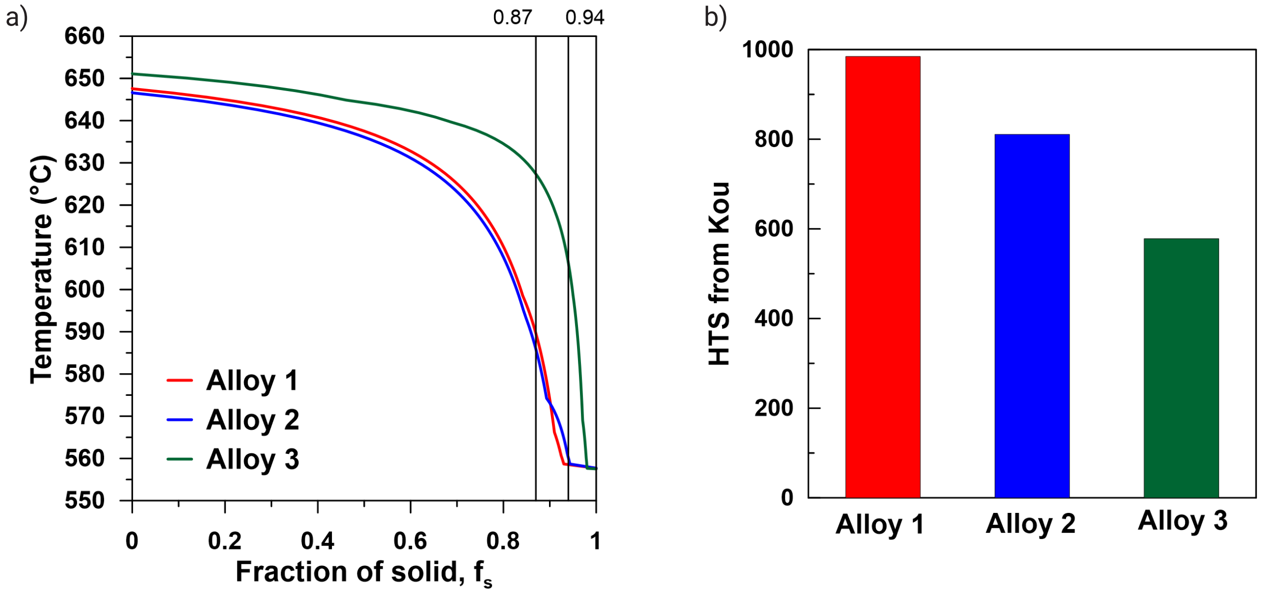

FIGURE 2: a) T vs. fs solidification paths calculated by Scheil's model; b) hot tearing susceptibility as predicted by Kou's model.

alloys are shown in Figure 3. From the visual inspection, it resulted that cracks tend to form across multiple branches for all the experimental alloys. In particular, for Alloy 1, all tests showed a complete ball separation in rod 1. As shown in the magnified views in Figure 3a, hairline cracks frequently appear at the ball end of rod 2, as well as the occurrence of severe cracks at the sprue area. In addition, light cracks were also detected at the sprue of rod 3. In Alloy 2 (Figure 3b), which registers a higher magnesium content, a slight improvement in crack resistance was observed. In all the castings from Alloy 2, a complete separation was noted near the ball end in rod 1 while severe crack occurred at the sphere of rod 2, while the sprue was always intact. Branch 3 also exhibited light cracking similar to that observed in the casting from Alloy 1. The best results were achieved with the castings produced using Alloy 3 (Figure 3c). In this case, cracks appeared primarily in the middle of branch 1, and light cracks observed at the sprue area of rod 2. Moreover, hairline cracks were found on the sprue of branch 3. No cracking was observed in rod 4, regardless of the alloy used.

The HTS values calculated in accordance with equation (1) are reported in the Figure 4 and analytically confirm the trends observed during visual inspection.

A comparative analysis of the histograms in Figure 2b and Figure 4 highlights a close match between the HTS values predicted using Kou's criterion and those experimentally determined from the CRC tests. This strong correlation validates the applicability of Kou's model as a reliable method for predicting the hot tearing susceptibility in aluminum alloys.

To further investigate the different behavior of the three alloys, microstructural analyses were conducted. Representative micrographs of the three alloys are reported in Figure 5. In all cases, the microstructures exhibit equiaxed dendritic grains with average grain sizes ranging from approximately 110 to 155 µm, as summarized in Table 2.

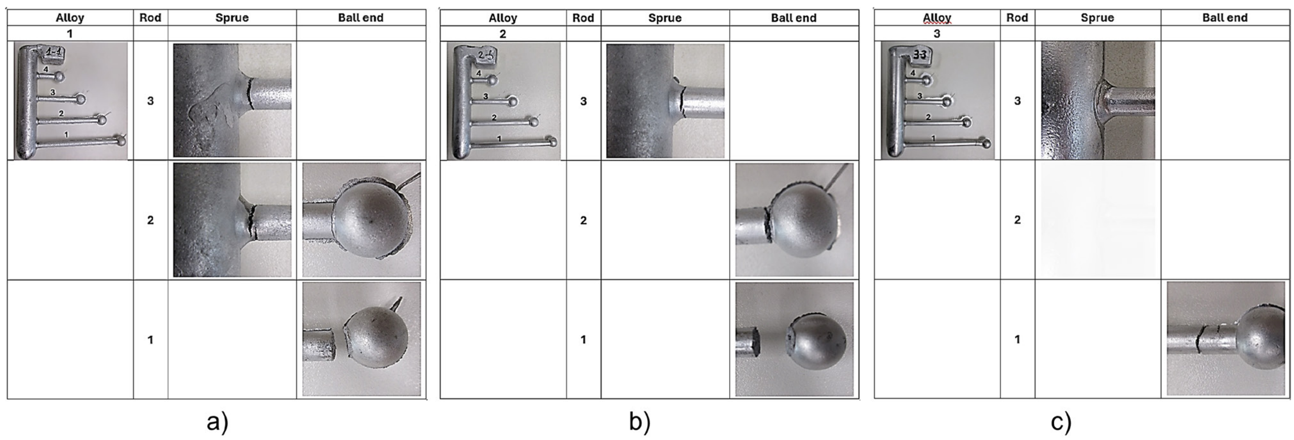

FIGURE 3: Castings from the CRC mold: a) Alloy 1; b) Alloy 2 and c) Alloy 3; in the inset, the close-up views of the tears near the sprue and ball-end of the rod.

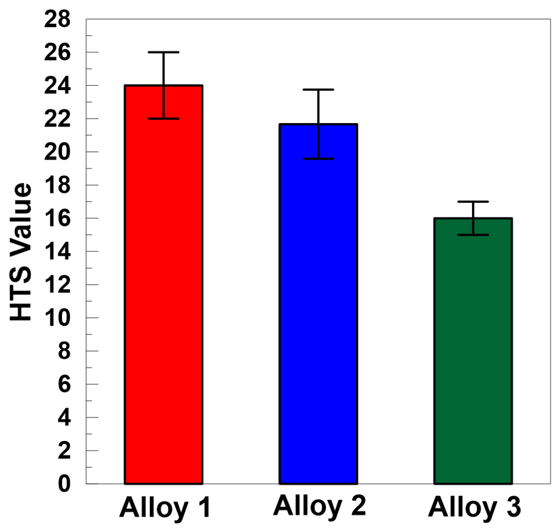

FIGURE 4: HTS values from the experimental CRC tests.

Nevertheless, no significant correlation was identified between grain size within this dimensional range and HTS values, suggesting that grain size is not a critical parameter in controlling hot tearing behavior. Consequently, more in-depth microstructural investigations were carried out.

Figure 6 presents SEM micrographs acquired in Z-contrast mode. EDS analyses (not shown) revealed the presence of β-Al_5FeSi as needle-like or plate-like brighter phases, and Mg_2Si, appearing as darker phases in Alloys 1 and 2 (Figure 6a and Figure 6b), both containing high levels of Si and Mg.

TABLE 2: Average grain size.

Alloy	Grain size (µm)
1	111 ± 7
2	154 ± 11
3	136 ± 10

It is worth noting that Alloy 2, with a slightly higher Mg concentration than Alloy 1, exhibited a greater density of these intermetallic compounds with a finer distribution. Additionally, Alloy 2 displayed a visibly smaller secondary dendrite arm spacing (SDAS) compared to Alloy 1.

Alloy 3, characterized by a high content of Fe and Mn and significantly lower concentrations of Si and Mg compared to the other two alloys, showed a high density of Chinese-script α-$Al_{15}(Fe,Mn)_3Si_2$ intermetallic compounds (Figure 6c), with no evidence of other phases. The addition of Mn in this alloy has induced a morphological transformation of the acicular β-Al_5FeSi phases, previously observed in the Mn-free alloys, into the more branched and interconnected α-$Al_{15}(Fe,Mn)_3Si_2$ structures. Moreover, Alloy 3 appears to exhibit even lower SDAS values than Alloy 2, further suggesting a refined solidification structure that may contribute to its lower hot tearing susceptibility.

Based on the SEM observations, it can be concluded that the reduction in hot tearing susceptibility may also be attributed to the size, morphology and solidification sequence of Fe-based intermetallic and eutectic phases. In particular, the α-$Al_{15}(Fe,Mn)_3Si_2$ phase seems to promote grain coalescence, facilitating bridging between primary dendrites and enhancing the structural integrity during

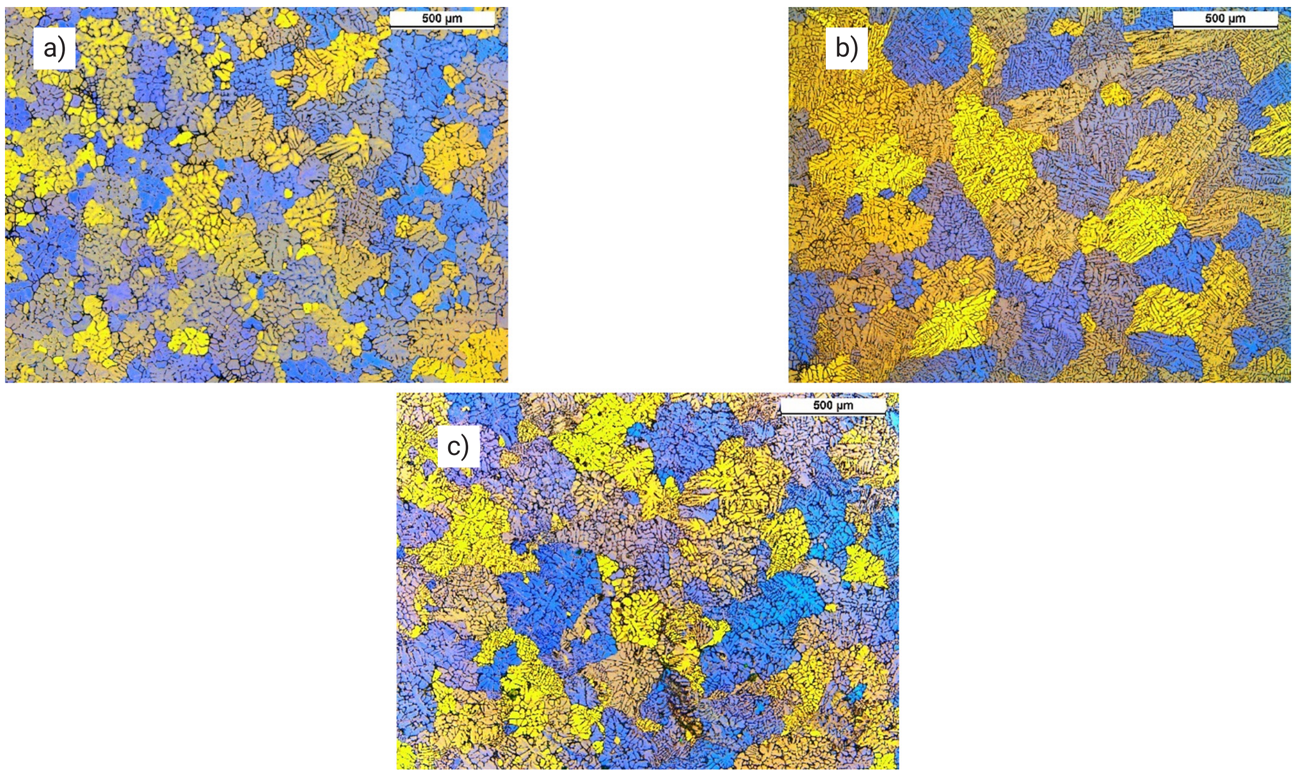

FIGURE 5: Optical micrographs showing the grain structure of a) Alloy 1, b) Alloy 2 and c) Alloy 3.

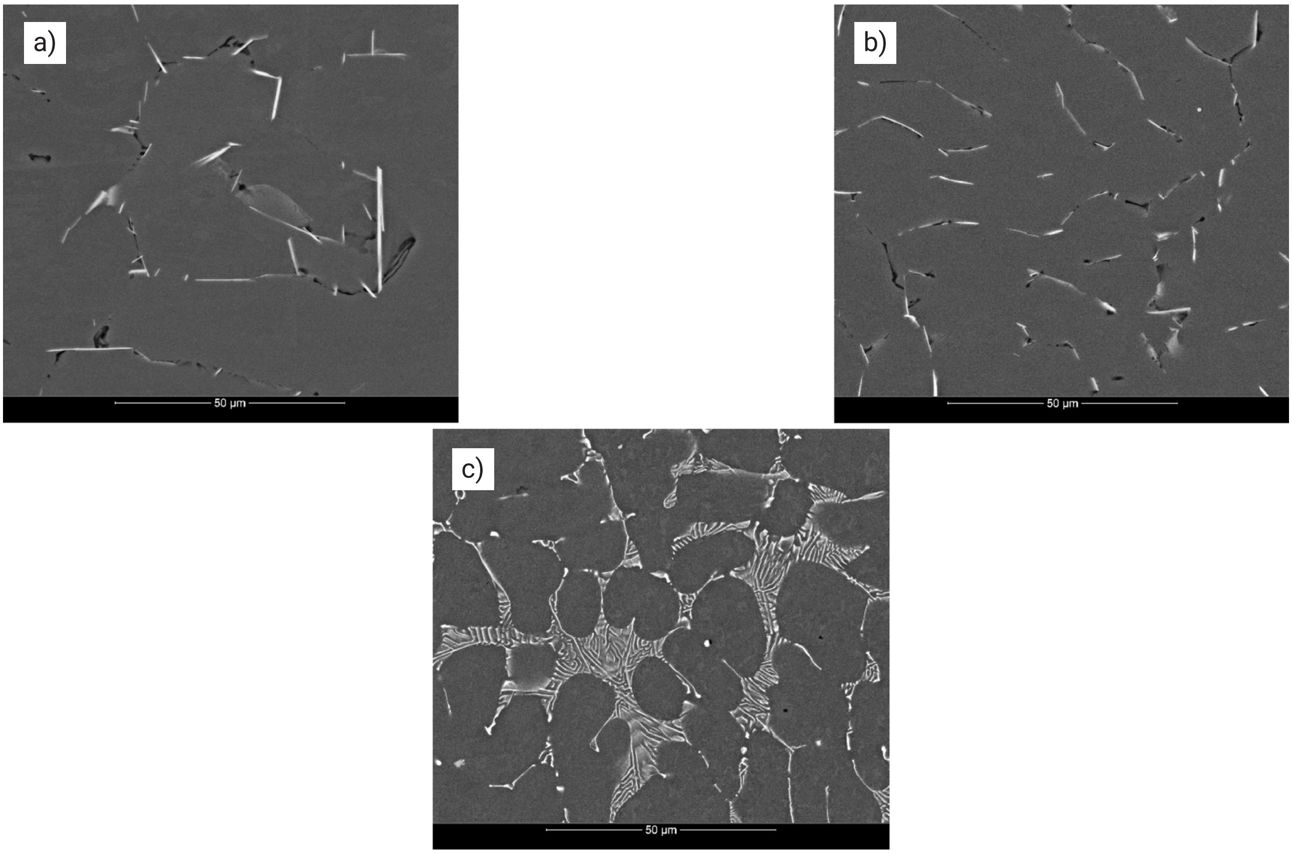

FIGURE 6: SEM micrographs of a) Alloy 1, b) Alloy 2 and 3) Alloy 3.

solidification and, finally, improving the castability of the alloy.

4. CONCLUSIONS

The castability of the 6XXX series alloys depends on their chemical composition. CRC testing has shown that the sensitivity to hot tears is higher in alloys with 0.2 wt% Fe and decreases with increased iron content. Improvements in hot tearing resistance are also associated with the presence of manganese, which changes the shape of iron rich intermetallic compounds promoting the formation of the α-$Al_{15}(Fe,Mn)_3Si_2$ phase. This phase acts as a reinforcement for the aluminum matrix and can enhance the bridging between grains.

Furthermore, the study suggests that thermodynamic simulation and the use of the Kou index can provide valuable insights into the casting of alloys. Experimental testing clearly matches the preliminary simulation results and shows the power of the proposed predictive model.

ACKNOWLEDGEMENTS

This study was carried out within the MICS (Made in Italy – Circular and Sustainable) Extended Partnership and received funding from the European Union Next-Generation EU (PIANO NAZIONALE DI RIPRESA E RESILIENZA (PNRR) – MISSIONE 4 COMPONENTE 2, INVESTIMENTO 1.3 – D.D. 1551.11-10-2022, PE00000004). This manuscript reflects only the authors' views and opinions, neither the European Union nor the European Commission can be considered responsible for them.

REFERENCES

Andersson, J., Helander, T., Höglund, L., Shi, P., & Sundman, B. (2002). Thermo-Calc and DICTRA, Computational Tools for Materials Science. Calphad, 26(2), 273-312. https://doi.org/10.1016/S0364-5916(02)00037-8

Cao, G., & Kou, S. (2006). Hot Craking of Binary Mg-Al Alloy Castings. Materials Science and Engineering A, 417, 230-238. https://doi.org/10.1016/j.msea.2005.10.050

Clyne, T., & Davies, G. (1975). A Quantitative Solidification Test for Casting and an Evaluation of Cracking in Aluminium-Magnesium Alloys. The British Foundrymen, 68, 238-244.

Cui, J., & Roven, H. (2010). Recycling of automotive aluminum. Transactions of nonferrous metals society of China, 2057-2063. https://doi.org/10.1016/S1003-6326(09)60417-9

https://doi.org/10.1007/978-3-319-51541-0 D'Errico, F., & Mattavelli, D. (2017). Secondary Aluminum Alloys Processed by Semisolid Process for Automotive Application. The Minerals, Metals & Materials Society, 227-234.

Dhale, A., & StJohn, D. (1998). Rheological Behaviour of the Mushy Zone and its Effect on the Formation of Casting Defects During Solidification. Acta Materialia, 47, 31-41. https://doi.org/10.1016/S1359-6454(98)00342-5

Eskin, D., Suytno, & Katgerman, L. (2004). Mechanical properties in the semi-solid state and hot tearing of aluminium alloys. Progress in Materials Science, 629-711. https://doi.org/10.1016/S0079-6425(03)00037-9

Ferro, P., & Bonollo, F. (2023). Lightweight design versus raw materials criticalities. Sustainable Materials and Technologies, 35, e00543. https://doi.org/10.1016/j.susmat.2022.e00543

Giansante, E., Timelli, G., & Fabrizi, A. (2024). Impact of Chemical Composition on Hot Tearing in Secondary Wrought Aluminum Alloys. Detritus, 29, 98-102. https://doi.org/10.31025/2611-4135/2024.19432

Giansante, E., Timelli, G., & Fabrizi, A. (2024). Influence of Chemical Composition on the Hot Tearing Susceptibility of Wrought 6005 Aluminum Alloys. Conference Proceedings- Metal 2024. Brno. https://doi.org/10.37904/metal.2024.4903

Graf, A. (2021). Chapter 3 - Aluminum alloys for lightweight automotive structures. In P. Mallick, Materials, Design and Manufacturing for Lightweight Vehicles (pp. 97-123). Elsevier Ltd. https://doi.org/10.1016/B978-0-12-818712-8.00003-3

Kou, S. (2015). A criterion for cracking during solidification. Acta Materialia, 88, 366-374. https://doi.org/10.1016/j.actamat.2015.01.034

Liang, K.-y., Huang, H.-C., Tseng, C.-Y., Chen, M.-C., Lee, S.-L., Lin, C.-C., & Su, T.-C. (2024). Effect of Fe, Si,Cu, and TiB2 Grain Refiner Amounts on the Hot Tearing Susceptibility of 5083, 6061, and 7075 Aluminum Ingots. Metals, 14(1). https://doi.org/10.3390/met14010015

Lin , S. (1999). A study of hot tearing in wrought aluminium alloys. Universitè du Québec à Chicoutimi. https://constellation.uqac.ca/id/eprint/1014/1/11716435.pdf

Phillion, A., Thompson, S., Crockcroft, S., & Wells, M. (2008). Tensile properties of as-cast aluminum alloys AA3104, AA6111 and CA31218 at above solidus temperatures. Materials Science and Engineering A, 497, 388-394. https://doi.org/10.1016/j.msea.2008.07.027

Polmear, I., StJohn, D., Nie, J.-F., & Quian, M. (2017). Light Alloys: Metallurgy of the Light Metals. Butterworth-Heinemann. ISBN: 008099430X, 9780080994307

Poznak, A., Freiberg, D., & Sanders, P. (2018). Chapter 10 - Automotive Wrought Aluminium Alloys. In Foundamentals of Aluminium Metallurgy_Recent Advances (pp. 333-386). Woodhead Publishing. https://doi.org/10.1016/B978-0-08-102063-0.00010-2

Raabe, D., Ponge, D., Uggowitzer, P., Roscher, M., Paolantonio, M., Liu, C., . . . Pogatscher, S. (2022). Making sustainable aluminum by recycling scrap: The science of “dirty” alloys. Progress in Materials Science, 128. https://doi.org/10.1016/j.pmatsci.2022.100947

Rajagukguk, K., Suyitno, S., Saptoadi, H., Kusumaningtyas, I., Aritvianto, B., Agus Salim, U., . . . Katgerman, L. (2024). Evaluation of Horizontal and Vertical Constrained Rod Casting Mold on Hot Tearing Susceptibility of Al-Cu Alloys. International Journal of Metalcasting, 18, 3329-3341. https://doi.org/10.1007/s40962-023-01250-z

Rappaz, M., Drezet, J.-M., & Gremaud, M. (1999). A new hot tearing criterion. Metallurgical and Materials Transactions A, 30A, 449-455. https://doi.org/10.1007/s11661-999-0334-z

Scheil, E. (1942). Bemerkungen zur schichtkristallbildung. International Journal of Materials Research, 34(3), 70-72.

TCAL7 Technical Information. (2020, 4 12). Retrieved 6 27, 2024, from https://www.engineering-eye.com/THERMOCALC/details/db/pdf/thermo-calc/02/TCAL7_technical_info.pdf

Uludag, M., Çetin, R., Dispinar , D., & Tiryakioglu, M. (2018). The effects of degassing, grain refinement & Sr-addition on melt quality-hot tear sensitivity relationship in cast A380 aluminum alloy. Engineering Failure Analysis, 90, 90-102. https://doi.org/10.1016/j.engfailanal.2018.03.025

Van den Eynde, S., Bracquen, E., Diaz-Romero, D., Zaplana, I., Engelen, B., Duflow, J. R., & Peters, J. R. (2022). Forecasting global aluminium flows to demonstrate the need for improved sorting and recycling methods. Waste Management(137), 231-240. https://doi.org/10.1016/j.wasman.2021.11.019